Commentary on "Tropospheric temperature response to stratospheric ozone recovery in the 21st century" by Hu et al.

Charles McLandress[1], Judith Perlwitz[2], and Theodore G. Shepherd[1]

[1]{Department of Physics, University of Toronto, Toronto, Ontario}

[2]{Cooperative Institute for Research in Environmental Sciences University of Colorado / NOAA Earth System Research Laboratory, Physical Sciences Division, Boulder, CO}

Correspondence to: C. McLandress (charles@atmosp.physics.utoronto.ca)

Abstract

In a recent paper Hu et al. (2011) suggest that the recovery of stratospheric ozone during the first half of this century will significantly enhance free tropospheric and surface warming caused by the anthropogenic increase of greenhouse gases, with the effects being most pronounced in Northern Hemisphere middle and high latitudes. These surprising results are based on a multi-model analysis of IPCC AR4 model simulations with and without prescribed stratospheric ozone recovery. Hu et al. suggest that in order to properly quantify the tropospheric and surface temperature response to stratospheric ozone recovery, it is necessary to run coupled atmosphere-ocean climate models with stratospheric ozone chemistry. The results of such an experiment are presented here, using a state-of-the-art chemistry-climate model coupled to a three-dimensional ocean model. In contrast to Hu et al., we find a much smaller Northern Hemisphere tropospheric temperature response to ozone recovery, which is of opposite sign. We argue that their result is an artifact of the incomplete removal of the large effect of greenhouse gas warming between the two different sets of models.

Introduction

Stratospheric ozone depletion has had a radiative effect on global mean surface climate, although the sign of the effect is uncertain due to the large compensation between the short-wave warming due to increased penetration of solar radiation and the long-wave cooling due to stratospheric cooling (Chapter 10 of SPARC CCMVal 2010). But all recent estimates (IPCC 2007, SPARC CCMVal 2010) are considerably less than 0.1 W/m^2, and thus represent a small number compared to the total radiative forcing. On the other hand, the Antarctic ozone hole, which is a huge perturbation to the Southern Hemisphere (SH) stratosphere, has been the dominant driver of past changes in high-latitude SH climate in summer (e.g. Arblaster and Meehl 2006, Fogt et al. 2009), with ozone recovery expected to offset the effects of climate change over the next half-century (e.g. Son et al. 2010). While similar physics might be expected to be at work at high latitudes in the Northern Hemisphere (NH), no such effect has so far been detected there, partly because of the smaller magnitude of ozone depletion in the Arctic, and partly because of the larger impact of greenhouse warming due to melting sea ice (see discussion in Chapter 4 of WMO 2011).

In a recent study, Hu et al. (2011; henceforth H11) investigated the possible impact of stratospheric ozone recovery on tropospheric temperatures using Intergovernmental Panel on Climate Change (IPCC) Fourth Assessment Report (AR4) general circulation model (GCM) simulations of the 21st century. They did this by comparing one set of model projections in which ozone recovery is prescribed with another set of projections (employing different models) in which ozone concentrations are held fixed, with both sets of projections having identical increases in well-mixed greenhouse gas (GHG) concentrations. Focusing on the period from 2001 to 2050, H11 find a significant enhancement of tropospheric warming in the GCM ensemble with prescribed ozone recovery. This enhanced warming is largest in the upper troposphere, with a global and annual mean change of ~0.41 K over 50 yrs (~0.08 K/decade). They also find relatively large enhanced warming in the extratropical and polar regions in summer and autumn in both hemispheres, as well as a significant warming at the surface with a global and

annual mean change of ~0.16 K over 50 yrs (~0.03 K/decade). In fact, the largest warming is found in the NH, which is very surprising given that the changes in stratospheric ozone are much larger in the SH. Furthermore the NH high-latitude surface warming maximizes in late fall/early winter, which is also very surprising since the ozone increase maximizes in spring. In addition, H11 compare their GCM results to results from a radiative-convective model, and find that although the latter predicts increased warming as ozone levels recover, the tropospheric warming is weaker by a factor of four than that determined from the ensembles of GCMs. They attribute this warming difference to the simplicity of their radiative-convective model.

Another possible explanation for the apparently large impact of stratospheric ozone recovery on NH temperatures is that their multi-model approach is flawed. Attributing differences between the two sets of simulations to the effects of ozone recovery is questionable if the signal one is looking for is small, as is the case for the impact of stratospheric ozone changes on tropospheric temperature everywhere outside the Antarctic. Since greenhouse warming is expected to dominate, small differences in the tropospheric temperature trends between the two sets of models may simply be a reflection of differences in the GHG-induced warming, and have nothing to do with ozone recovery. Although H11 claim that the mean transient climate response (TCR) of the two sets of models is the same (1.7 K), we compute a difference of 0.22 K for the models used for the future changes, based on the incomplete information provided in Table 8.2 of IPCC (2007). It is therefore plausible that a relatively small difference in the mean TCRs could account for the different rates of tropospheric warming in their two sets of model simulations. Furthermore, the rate of Arctic warming, which is not encapsulated in a global metric like the TCR, also differs from model to model because of different rates of Arctic sea ice loss. In fact, Crook and Forster (2011) show that GCMs with large Arctic amplification factors do not necessarily have large TCRs. Thus, even if the mean TCRs of the two sets of models were identical, the mean Arctic amplification factors will almost certainly differ. The enhanced surface warming in Arctic winter found by H11 for the models with imposed ozone recovery may therefore be a reflection of that.

In their Conclusion, H11 acknowledge the limitations in their approach and suggest that coupled atmosphere-ocean models including stratospheric ozone chemistry are needed to properly investigate the tropospheric and surface temperature responses to stratospheric ozone recovery, in order to avoid this "small differences of large terms" problem. Here, we describe results from such an exercise, using simulations from the Canadian Middle Atmosphere Model (CMAM). By comparing an ensemble of simulations with increasing GHG concentrations and time-varying ozone-depleting substances (ODSs) to an ensemble of simulations with only increasing GHG concentrations (i.e., ODS concentrations held fixed), using the same coupled model, we are able to assess the impact of ozone recovery on tropospheric temperatures in a self-consistent manner. Contrary to the results of H11, we find only a small NH tropospheric temperature response to ozone recovery, which is in fact opposite in sign to theirs.

The outline of our paper is as follows. In Section 2 we describe CMAM and the simulations we use. In Section 3 we discuss our results. For easy comparison we present many of our results in a similar format to that used by H11. In Section 4 we discuss in greater depth the potential causes for the disagreement between our results and those of H11.

1 Description of model and simulations

CMAM is the upward extension of the Canadian Centre for Climate Modelling and Analysis (CCCma) third generation coupled GCM (CGCM3). The ocean component of CMAM is described in McLandress et al. (2010). The atmospheric component has 71 vertical levels, with a resolution that varies from several tens of meters in the lower troposphere to ~2.5 km in the mesosphere. A T31 spectral resolution is used in the horizontal, which corresponds to a grid spacing of ~6°. Detailed descriptions of the stratospheric chemistry scheme and the atmospheric component of CMAM are provided in de Grandpré et al. (2000) and Scinocca et al. (2008), respectively.

The two sets of simulations we use are described in detail in McLandress et al. (2010), and the evolution of ozone in the simulations is described in Plummer et al. (2010). The

first set is the "REF-B2" simulation, which employs time varying concentrations of GHGs and ODSs, with the GHGs prescribed according to the moderate SRES A1B scenario (IPCC 2001) and the ODSs according to the A1 scenario (WMO 2007). The second set is the "GHG" simulation in which the concentrations of GHGs used in the radiation scheme are allowed to vary in time as in REF-B2, but the concentrations of ODSs are held fixed at their 1960 values in the chemistry scheme. Note that in the GHG simulation time-varying concentrations of CFC-11 and CFC-12 are used in the radiation scheme, as in the REF-B2 simulation. The impact of the ODS changes (and therefore the impact of the stratospheric ozone changes) is inferred by differencing the REF-B2 and GHG simulations, as in Plummer et al. (2010). The simulations extend from 1960 to 2099, with each set of simulations comprising an ensemble of three. Details of the spin-up procedure are given in McLandress et al. (2010).

We present results both for the 1960-2000 ("ozone depletion" or "past") period and the 2001-2050 ("ozone recovery" or "future") period. Since the sign of the trends driven by changes in stratospheric ozone is expected to change from past to present (e.g., McLandress et al. 2010, 2011), comparing these two periods helps in assessing the robustness of the results. Linear trends are computed from ensemble mean time series, and their statistical significance is computed using the standard t-test (i.e., assuming independent and Gaussian-distributed residuals). All figures show ensemble averages.

2 Results

2.1 Annual mean

Figure 1 shows latitude-height sections of annual and zonal mean temperature trends for the REF-B2 (left) and GHG (middle) simulations and their difference (right) for the past (top) and future (bottom). REF-B2 and GHG both show tropospheric warming and stratospheric cooling over both periods as a result of increasing GHG concentrations in those two simulations. The difference between the two shows large statistically significant trends in the SH polar stratosphere, which change sign from past to future as

the Antarctic ozone hole recovers. In the troposphere there are several regions of statistically significant trends in the future, with weak warming at high Southern latitudes and cooling in the Arctic. Although the tropospheric temperature trends are not statistically significant in the past, they are of opposite sign to the future trends. The lower right panel in Fig. 1 is directly comparable to Fig. 6a of H11. In contrast to their results, we see no evidence of enhanced tropospheric warming during the ozone recovery period, and, as stated above, we in fact find weak cooling in the NH.

A more compact way of presenting the annual mean temperature trends is by plotting latitudinal averages, as is done in Fig. 2. Shown here are global averages (left), SH average (middle) and NH average (right) for REF-B2 (black), GHG (blue) and REF-B2 minus GHG (red) for the past and future. The two left and bottom right panels are directly comparable to Figs. 2 and 4 of H11. The maximum impact of the ozone changes occurs at ~70 hPa, with the effect being much larger in the SH than in the NH, as expected. We also note that the magnitude of the trends in REF-B2 minus GHG is larger for the past than for the future because the ozone recovery process is not completed by 2050 (Plummer et al. 2010).

Closer inspection of the right panels of Fig. 2 reveals that below about 300 hPa the 95% uncertainty error bars on the red curve do not cross the zero line, indicating that there is a statistically significant impact of both ozone depletion and ozone recovery on NH average tropospheric temperature. Interestingly, our model results suggest that NH ozone depletion has led to a small tropospheric warming, which would be consistent with ozone depletion exerting a net positive forcing (Chapter 10 of SPARC CCMVal 2010). Our simulations also suggest that ozone recovery will lead to a small tropospheric cooling. However, both the past and future NH tropospheric temperature trends are small (~0.02 K/decade in the upper troposphere, i.e., about a factor of four smaller than the future warming found by H11).

Time series of the annual mean temperatures for REF-B2 and GHG (left) and their difference (right) are shown in Fig. 3. The top panel shows global means at 50 hPa. The temperatures remain nearly the same up until about 1980, when they start to diverge,

reaching their largest differences near year 2000, after which they begin to slowly converge, as is more clearly seen in the difference plot to the right. This behavior is what is expected from the ODS-induced changes in ozone. Global mean temperatures at 300 hPa (middle), as well as in the tropics at 200 hPa (bottom), exhibit the steady warming due to increasing GHGs, but no significant difference between REF-B2 and GHG. However there appears to be a weak warming in the past and cooling in the future, consistent with the NH average behavior shown in Fig. 2. Both the magnitude and the sign of the effect are contrary to the significantly enhanced tropospheric warming in the 2001-2050 period found by H11.

2.2 Seasonal variation

Turning now to the seasonal variation of the ODS-induced temperature changes in the troposphere, the left panels in Fig. 4 show latitude-month cross sections of the REF-B2 minus GHG temperature trends at 300 hPa. Opposite-signed trends between past and future are seen at high Southern latitudes in late spring and early summer. These are due to the delayed breakdown of the SH vortex during the ozone depletion period and the return to earlier breakdown dates during the ozone recovery period (e.g. McLandress et al. 2010). Comparing the bottom left panel to Fig. 8a in H11, one can clearly see the above-mentioned SH features in the AR4 model results. However, the warming at low and middle latitudes in the NH in summer seen in H11 is absent in our results. Although there are patches of past warming and future cooling in the NH, which are consistent with the NH average results shown in Fig. 2, they are not statistically significant when considered regionally and seasonally. The top panels of Fig. 5 show time series at 300 hPa averaged from 30°N to 90°N and from June to October, the time period H11 found to exhibit the largest enhanced warming. The trends in Fig. 5 are not statistically significant, and, as was seen in Fig. 3, show, if anything, future cooling as opposed to the future warming found by H11.

H11 also found large enhanced surface warming in the Arctic during the period of ozone recovery, and suggested that the increasing ozone concentrations are somehow amplifying the high-latitude response to global warming. The right panels of Fig. 4 show

the zonal mean temperature trends at the surface. A comparison of the bottom right panel to Fig. 11 of H11 reveals major differences. H11 reported strong warming in the Arctic, especially in fall and winter, while CMAM shows cooling at these latitudes. The CMAM time series of the Arctic surface temperature average from September to January (bottom panels of Fig. 5) — the time period H11 found to exhibit the maximum warming — exhibit strong inter-annual variability, which explains the lack of statistical significance in this region and season in Fig. 4.

3 Conclusions and Discussion

A self-consistent analysis of the possible impact of stratospheric ozone recovery on tropospheric temperatures has been undertaken using a version of the Canadian Middle Atmosphere Model (CMAM) that is coupled to an ocean model. Two sets of simulations are performed: one with time-varying concentrations of GHGs and ODSs, the other with time-varying GHGs and constant ODSs. Although our simulations show the expected large differences in stratospheric temperature changes, we find only a small impact on tropospheric temperatures, consistent with the small estimated radiative forcing of stratospheric ozone changes (IPCC 2007, SPARC CCMVal 2010). Interestingly, the effect in the NH is such that ozone depletion leads to a tropospheric warming, and ozone recovery to a tropospheric cooling, which is consistent with ozone depletion representing a positive radiative forcing as has been suggested in recent studies (SPARC CCMVal 2010).

Our results are in stark contrast to those of Hu et al. (2011), who suggest that ozone recovery will have a substantial warming effect in the troposphere [a global and annual mean change of ~0.41 K over 50 yrs (~0.08 K/decade) in the upper troposphere, compared with the cooling of ~0.02 K/decade found here], which is largest in the NH. H11 base their findings on an analysis of IPCC AR4 models with and without ozone recovery. This approach has been used successfully to determine the impact of stratospheric ozone changes on SH summertime circulation changes (e.g., Perlwitz et al. 2008, Fogt et al. 2009, Son et al. 2009), as confirmed by a multi-model comparison of

CCMVal models (e.g., Son et al. 2010) and sensitivity studies using single models (McLandress et al. 2011, Polvani et al. 2011). The reason why this approach works in the summertime SH is because the Antarctic ozone hole is such a large perturbation to the SH circulation. However, applying such an analysis to the NH, in particular the Arctic, as H11 do, is problematic since the stratospheric ozone changes in northern high latitudes are considerably weaker, and the GHG-induced warming (which needs to be removed in order to isolate the effects of ozone recovery) is larger.

We argue that the enhanced tropospheric warming found by H11 results from the comparison of groups of models having different climate sensitivities; specifically, that differencing the two groups of models does not remove the effect of GHG-induced warming as is needed in order to isolate the effects of ozone recovery. Important regions where such sensitivity to GHG changes becomes obvious are the upper tropical troposphere and the Arctic surface. The rate of upper tropical tropospheric warming is closely related to the rate of surface warming (Arblaster et al. 2011), which is closely linked to the climate sensitivity of the model. For the Arctic, surface warming is strongly determined by the rate of Arctic sea ice loss. Stroeve et al. (2007) showed that AR4 models exhibit a large range of declining sea ice extent trends for the period 1953-2006. Thus, compositing two model sets with different sea ice loss rates will result in large apparent effects in Arctic surface temperatures. The seasonality of the Arctic warming determined by H11, with maximum surface warming during late fall/early winter, is consistent with the seasonality expected from the impact of Arctic sea ice loss (Deser et al. 2010). This seasonality is not consistent with the effect of stratospheric ozone changes, which maximize in spring.

We provide here a simple yet illustrative demonstration of why the method of H11 is inappropriate in the tropical and NH troposphere where the impact of ozone forcing is expected to be small relative to that of other processes. We do this by computing differences in two ensembles of simulations produced using two different versions of CMAM. The first is the "REF2" simulation generated using the CCMVal-1 version of CMAM (Eyring et al. 2007). Like REF-B2, the REF2 ensemble of three simulations uses time-varying concentrations of GHGs and ODSs, but unlike REF-B2 it employs

prescribed sea-surface temperatures and sea-ice distributions generated using an earlier version of the CCCma coupled atmosphere-ocean model on which that version of CMAM was based. The second set is the GHG simulation using the CCMVal-2 version of CMAM, which has been discussed above. Differencing the two ensemble means is thus analogous to H11 differencing the means of the two different sets of AR4 models with and without ozone recovery.

The results of this exercise are given in Fig. 6, which shows annual and zonal mean temperature trends for the 2001-2050 period for the two sets of simulations and for the corresponding difference. As with the REF-B2-GHG differences shown previously (bottom right panel in Fig. 1), the impact of ozone recovery is clearly seen in the Antarctic lower stratosphere. However, large statistically significant trends (cooling) are also found in the troposphere, with larger values in the NH than in the SH and with a strong surface signal in the Arctic, much as in H11 but of opposite sign. The reason why there are such large differences in the troposphere is because the GHG-induced warming is stronger in the CCMVal-2 version of CMAM than in the CCMVal-1 version, with tropical (20°S to 20°N) sea-surface temperature trends from 2001-2050 of ~ 0.27 K/decade and 0.20 K/decade, respectively. Thus, differencing the two sets of simulations yields the cooling trends seen in the right panel of Fig. 6. The fact that H11 find enhanced warming, while Fig. 6 shows cooling, is immaterial since the mean rate of GHG-induced global warming in the AR4 models with ozone recovery may simply be larger than in those without. Note that we are unable to confirm H11's claim that the transient climate responses (TCR) of the two sets of AR4 models was the same. Based on Table 1 in H11 and the incomplete information in Table 8.2 in IPCC (2007) where TCRs for 5 of the 21 models used by H11 for the 21st century projections were not available, we compute mean values of 1.93 and 1.71 K for the AR4 models with and without ozone recovery, respectively. Differencing the two TCRs yields a positive value, which is consistent with the enhanced tropospheric warming found by H11 for the models with imposed ozone recovery.

While our results are for only a single model (and so are subject to the potential weaknesses of that model), they clearly show the dangers in analysing AR4 models with

and without ozone recovery when trying to quantify the impacts of ozone recovery on tropospheric temperatures in the NH. A more definitive analysis would require a multi-model approach using coupled chemistry-climate models or IPCC-like models in which each model performs simulations with and without ozone recovery, and where the ocean and sea ice models coupled to the atmospheric model can respond.

Acknowledgements

The CMAM simulations analysed here were produced by the C-SPARC project with funding from the Canadian Foundation for Climate and Atmospheric Sciences. Computing support and funding for CM was provided by Environment Canada. JP acknowledges support from the NASA Modeling and Analysis Program.

References

Arblaster, J. M., Meehl, G. A., and Karoly, D. J.: Future climate change in the Southern Hemisphere: Competing effects of ozone and greenhouse gases, Geophys. Res. Lett., 38, L02701, doi:10.1029/2010GL045384, 2011.

Arblaster, J. M., and Meehl, G. A.: Contributions of external forcings to southern annular mode trends, J. Climate, 19, 2896-2904, 2006.

Crook, J. A., and Forster, P. M.: A balance between radiative forcing and climate feedback in the modeled 20th century temperature response, J. Geophys. Res., 116, D17108, doi:10.1029/2011JD015924, 2011.

Deser, C., Tomas, R., Alexander, M., and Lawrence, D.: The seasonal atmospheric response to projected Arctic sea ice loss in the late 21st century. J. Climate, 23, 333-351, 10.1175/2009JCLI3053.1, 2010.

Eyring, V., et al.: Multimodel projections of stratospheric ozone in the 21st century, J. Geophys. Res., 112, D16303, doi:10.1029/2006JD008332, 2007.

Fogt, R. L., Perlwitz, J., Monaghan, A. J., Bromwich, D. H., Jones, J. M., and Marshall, G. J.: Historical SAM Variability. Part II: Twentieth-Century Variability and Trends from Reconstructions, Observations, and the IPCC AR4 Models. J. Climate, 22, 5346-5365, 2009.

de Grandpré, J., Beagley, S. R., Fomichev, V. I., Griffioen, E., McConnell, J. C., Medvedev, A. S., and Shepherd, T. G.: Ozone climatology using interactive chemistry: Results from the Canadian middle atmosphere model. J. Geophys. Res., 105, 26475-26491, 2000.

Hu, Y., Xia, Y., and Fu, Q.: Tropospheric temperature response to stratospheric ozone recovery in the 21st century, Atmos. Chem. Phys., 11, 7687-7699, doi:10.5194/acp-11-7687-2011, 2011.

Intergovernmental Panel on Climate Change (IPCC): Climate Change 2007: The Physical Scientific Basis: Contribution of Working Group I to the Fourth Assessment Report of the Intergovernmental Panel on Climate Change, Edited by Solomon, S., Qin, D., Manning, M., Chen, Z., Marquis, M., Averyt, K.B., Tignor, M., and Miller, H.L., Cambridge University Press, New York, 996 pp., 2007.

Intergovernmental Panel on Climate Change (IPCC): Climate Change 2001: The Scientific Basis: Contribution of Working Group I to the Third Assessment Report of the Intergovernmental Panel on Climate Change, edited by J. T. Houghton et al., Cambridge University Press, New York, 881 pp., 2001.

McLandress, C., Jonsson, A. I., Plummer, D. A., Reader, M. C., Scinocca, J. F., and Shepherd, T. G.: Separating the dynamical effects of climate change and ozone depletion: Part 1. Southern Hemisphere Stratosphere. J. Climate, 24, 1850–1868, 2010.

McLandress, C., Shepherd, T. G., Scinocca, J. F., Plummer, D. A., Sigmond, M., Jonsson, A. I., and Reader, M. C.: Separating the dynamical effects of climate change and ozone depletion: Part 2. Southern Hemisphere Troposphere. J. Climate, 23, 5002-5020, doi: 10.1175/2010JCLI3586.1, 2011.

Perlwitz, J., Pawson, S., Fogt, R. L., Nielsen, J. E., and Neff, W. D.: Impact of stratospheric ozone hole recovery on Antarctic climate. Geophys. Res. Lett., 35, L08714, doi:10.1029/2008GL033317, 2008.

Plummer, D. A., Scinocca, J. F., Shepherd, T. G., Reader, M. C., and Jonsson, A. I.: Contributions to stratospheric change from ozone depleting substances and greenhouse gases. Atmos. Chem. Phys., 10, 9647-9694, doi:10.5194/acpd-10-9647-2010, 2010.

Polvani, L. M., Previdi, M., and Deser, C.: Large cancellation, due to ozone recovery, of future Southern Hemisphere atmospheric circulation trends, Geophys. Res. Lett., 38, L04707, doi:10.1029/2011GL046712, 2011.

Scinocca, J. F., McFarlane, N. A., Lazare, M., Li, J., and Plummer, D.: The CCCma third generation AGCM and its extension into the middle atmosphere. Atmos. Chem. Phys., 8, 7055-7074, 2008.

Son, S.-W., et al.: Impact of stratospheric ozone on Southern Hemisphere circulation change: A multimodel assessment, J. Geophys. Res., 115, D00M07, doi:10.1029/2010JD014271, 2010.

Son, S.-W., Tandon, N. F., Polvani, L. M., and Waugh D. W.: Ozone hole and Southern Hemisphere climate change, Geophys. Res. Lett., 36, L15705, doi:10.1029/2009GL038671, 2009.

SPARC CCMVal Report on the Evaluation of Chemistry-Climate Models: Eyring, V., Shepherd, T. G., and Waugh, D. W. (Eds.), SPARC Report No. 5, WCRP-132, WMO/TD-No. 1526, http://www.atmosp.physics.utoronto.ca/SPARC, 2010.

Stroeve, J., Holland, M., Meier, W., Scambos, T., and Serreze, M.: Arctic sea ice decline: Faster than forecast, Geophys. Res. Lett., 34, L09501, doi:10.1029/2007GL029703, 2007.

World Meteorological Organization (WMO)/United Nations Environment Programme

(UNEP), 2006: Scientific assessment of ozone depletion, Global Ozone Res. Monit. Proj. Rep., 50, WMO, Geneva, Switzerland, 2007.

WMO (World Meteorological Organization), Scientific Assessment of Ozone Depletion: 2010, Global Ozone Research and Monitoring Project–Report No. 52, 516 pp., Geneva, Switzerland, 2011.

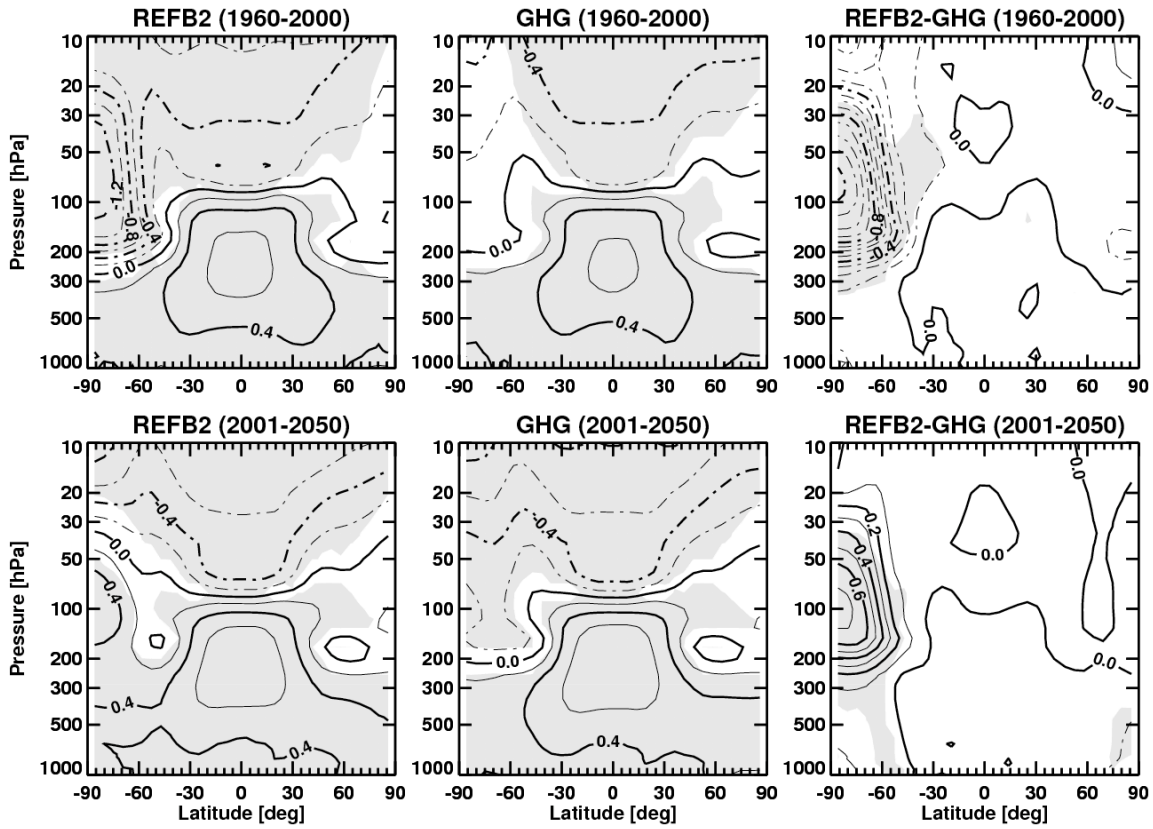

Figure 1. Annual and zonal mean temperature trends for 1960-2000 (top) and 2001-2050 (bottom): REF-B2 (left), GHG (middle), and REF-B2 minus GHG (right). Contour intervals are 0.2 and 0.1 K/decade in the two left columns and right columns, respectively. Shading denotes regions where the 95% significance level is exceeded.

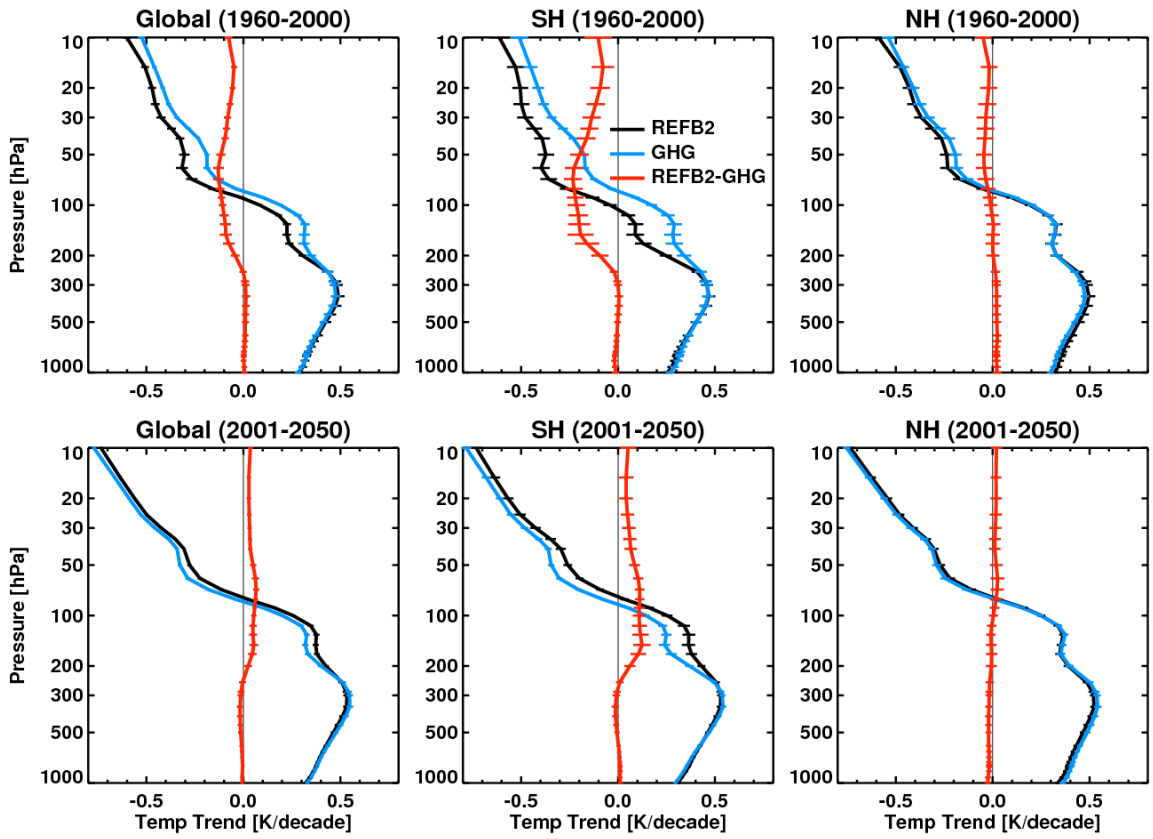

Figure 2. Annual mean temperature trends for 1960-2000 (top) and 2001-2050 (bottom): global average (left), Southern Hemisphere (middle) and Northern Hemisphere (right) for REF-B2 (black), GHG (blue) and REF-B2 minus GHG (red). Error bars denote the 95% confidence levels of the trends.

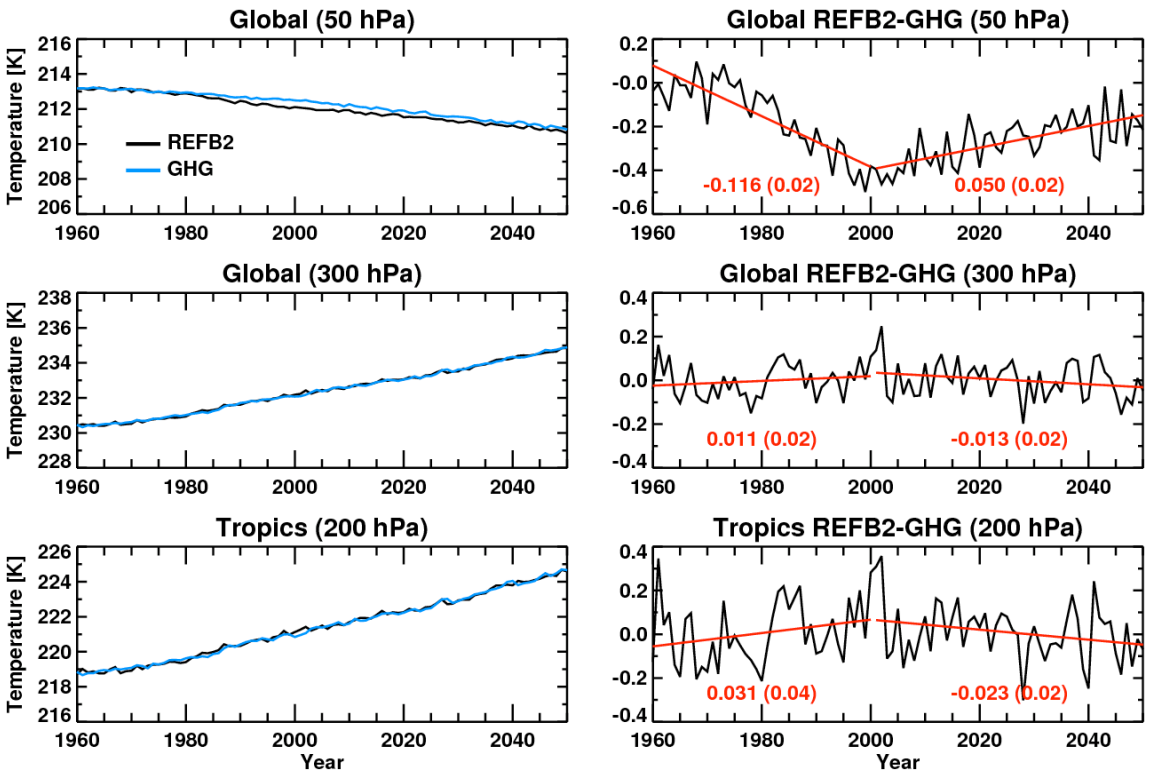

Figure 3: Annual mean temperature time series: global average at 50 hPa (top), global average at 300 hPa (middle) and tropical average (20°S-20°N) at 200 hPa (bottom). Left panels show REF-B2 (black) and GHG (blue); right panels show REF-B2 minus GHG (black) and the corresponding linear trends and 95% uncertainties (in brackets) for 1960-2000 and 2001-2050 in K/decade.

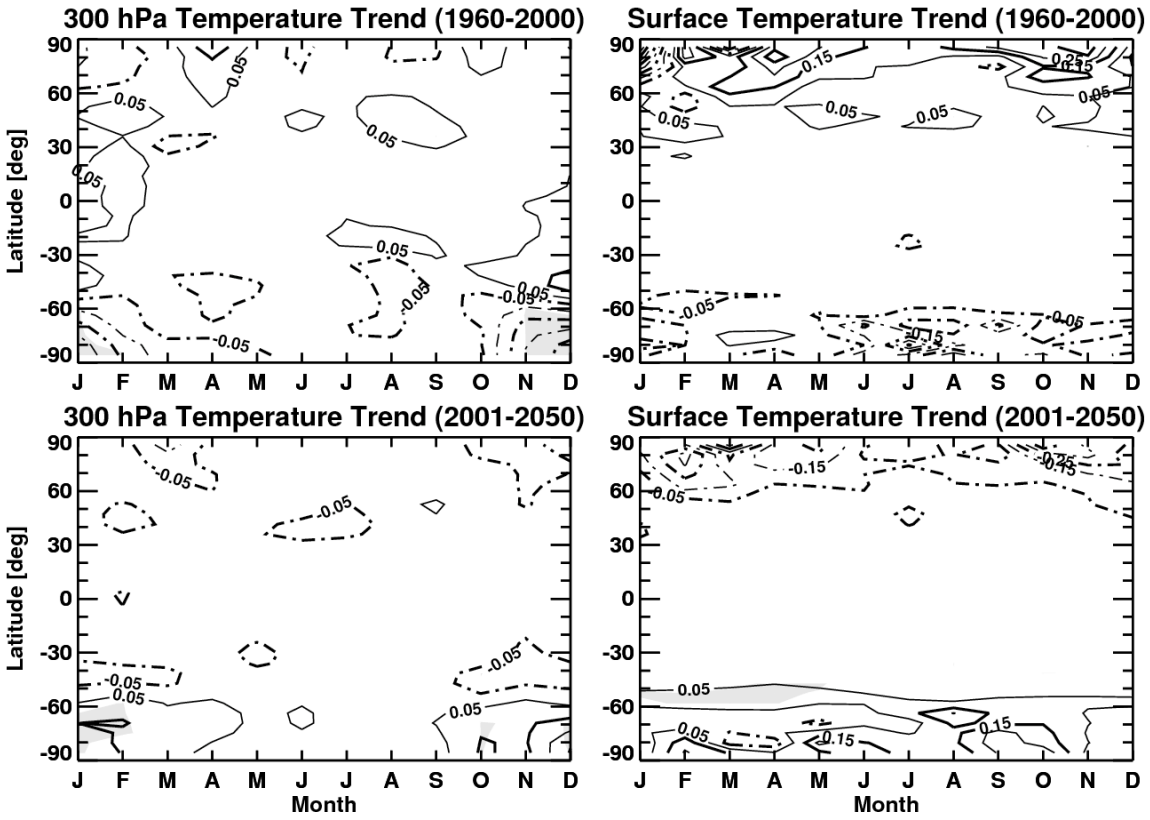

Figure 4: Zonal mean temperature trend versus month and latitude for REF-B2 minus GHG for 1960-2000 (top) and 2001-2050 (bottom) at 300 hPa (left) and at the surface (right). Contour interval is 0.1 K/decade. Shading denotes regions where the 95% significance level is exceeded.

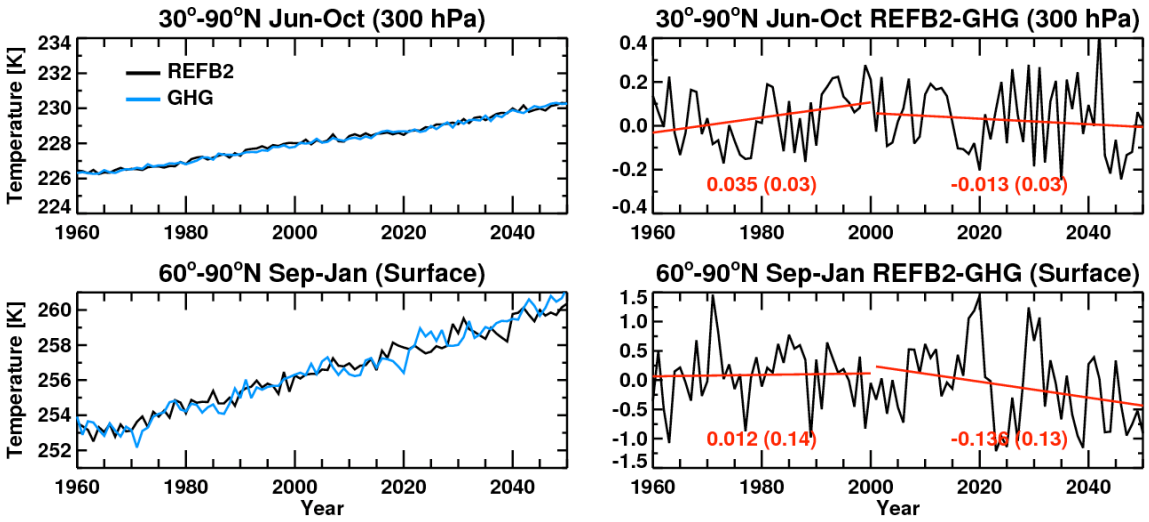

Figure 5: (Top) Temperature time series at 300 hPa averaged from 30°N-90°N for June to October: (left) REF-B2 (black) and GHG (blue); (right) REF-B2 minus GHG (black) and the corresponding linear trends (K/decade) and 95% uncertainties (in brackets) for 1960-2000 and 2001-2050 in K/decade. Bottom: same as top panels but for surface air temperature averaged from 60°N-90°N for September to January.

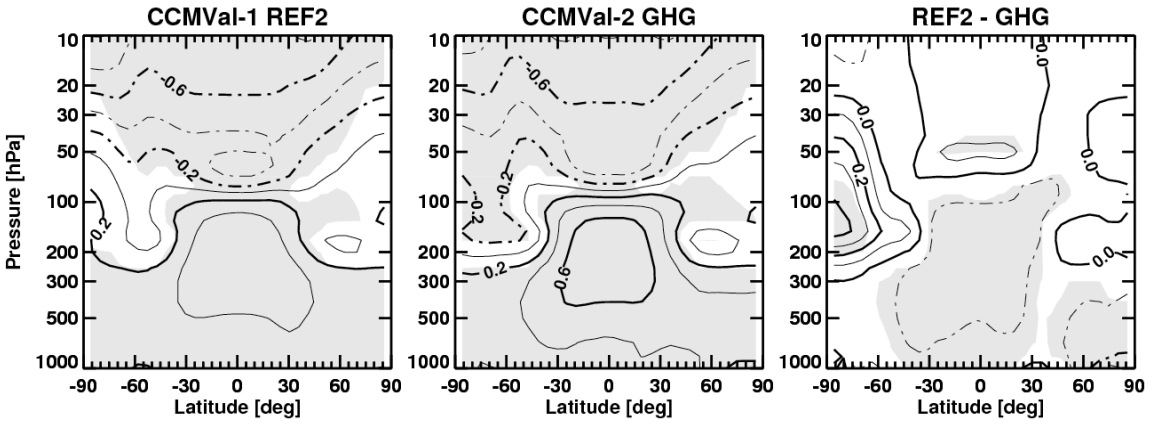

Figure 6: Annual and zonal mean temperature trends for 2001-2050: CCMVal-1 REF2 (left), CCMVal-2 GHG (middle), and CCMVal-1 REF2 minus CCMVal-2 GHG (right). Contour intervals are 0.2 and 0.1 K/decade in the two left panels and the right panel, respectively. Shading denotes regions where the 95% significance level is exceeded.